



PII S0016-7037(02)00901-8

Carbon isotope evidence implying high O₂/CO₂ ratios in the Permo-Carboniferous atmosphere

D. J. BEERLING,¹ J. A. LAKE,^{1,*} R. A. BERNER,² L. J. HICKEY,² D. W. TAYLOR³ and D. L. ROYER^{1,2}¹Department of Animal and Plant Sciences, University of Sheffield, Sheffield S10 2TN, UK²Department of Geology and Geophysics, Yale University, New Haven, CT 06520-8109, USA³Department of Biology, Indiana University Southeast, New Albany, IN 47150, USA

(Received September 10, 2001; accepted in revised form March 19, 2002)

Abstract—Theoretical models predict a marked increase in atmospheric O₂ to ~35% during the Permo-Carboniferous (~300 Ma) occurring against a low (~0.03%) CO₂ level. An upper O₂ value of 35%, however, remains disputed because ignition data indicate that excessive global forest fires would have ensued. This uncertainty limits interpretation of the role played by atmospheric oxygen in Late Paleozoic biotic evolution. Here, we describe new results from laboratory experiments with vascular land plants that establish that a rise in O₂ to 35% increases isotopic fractionation (Δ¹³C) during growth relative to control plants grown at 21% O₂. Despite some effect of the background atmospheric CO₂ level on the magnitude of the increase, we hypothesize that a substantial Permo-Carboniferous rise in O₂ could have imprinted a detectable geochemical signature in the plant fossil record. Over 50 carbon isotope measurements on intact carbon from four fossil plant clades with differing physiological ecologies and ranging in age from Devonian to Cretaceous reveal a substantial Δ¹³C anomaly (5‰) occurring between 300 and 250 Ma. The timing and direction of the Δ¹³C excursion is consistent with the effects of a high O₂ atmosphere on plants, as predicted from photosynthetic theory and observed in our experiments. Preliminary calibration of the fossil Δ¹³C record against experimental data yields a predicted O₂/CO₂ mixing ratio of the ancient atmosphere consistent with that calculated from long-term models of the global carbon and oxygen cycles. We conclude that further work on the effects of O₂ in the combustion of plant materials and the spread of wildfire is necessary before existing data can be used to reliably set the upper limit for paleo-O₂ levels. Copyright © 2002 Elsevier Science Ltd

1. INTRODUCTION

Oxygen is a fundamental atmospheric constituent influencing the metabolism and ecology of many groups of terrestrial and marine aerobic organisms. On a time scale of millions of years, its partial pressure (*p*O₂) is determined by regulatory feedback mechanisms (Holland, 1978), but the nature and action of these mechanisms in the Phanerozoic (past 550 Ma) remain areas of extensive debate (Robinson, 1989; Berner, 1999; Lenton and Watson, 2000). The ~350 Ma continuous record of fossil charcoal indicates that atmospheric oxygen probably never fell below one third of the present atmospheric level (Cope and Chaloner, 1980), but the upper limit is less securely determined. Geochemical models based on the abundance of organic carbon and pyritic sulfur in sedimentary rocks indicate a relatively stable O₂ value through the past 550 Ma but with a major excursion up to 35% in the Permo-Carboniferous (Berner and Canfield, 1989). This feature of O₂ evolutionary history has been closely reproduced by an independent mass balance approach using geologic records of the isotopic composition of sedimentary carbonates and sulfates (Berner et al., 2000; Berner, 2001). Nevertheless, an upper O₂ limit of ~35% appears incompatible with some experimental combustion data (Watson et al., 1978; Lenton and Watson, 2000). These data indicate that at no time in the Phanerozoic could O₂ have been greater than 25%, since it would have led to the spontaneous ignition of terrestrial vegetation and widespread

forest fires (Watson et al., 1978), a prediction not apparent in the paleorecord of wildfires. However, the ignition data were determined only from paper strips, and their relevance to actual forest fires has been questioned (Robinson, 1989).

The upper O₂ limit during the Permo-Carboniferous continues to remain controversial, and new approaches are required to address this issue. One potentially useful line of research is the analysis of the isotopic composition of fossil plants. In plants with the C₃ photosynthetic pathway, discrimination against the heavy isotope of carbon (Δ¹³C) is linked to leaf gas exchange processes via a well-validated theoretical model (Farquhar et al., 1982; Farquhar and Lloyd, 1993) according to:

$$\Delta^{13}\text{C} = a + (b - a) \times \frac{p_i}{p_a}, \quad (1)$$

where *a* is the fractionation that occurs during diffusion through the stomata (4.4‰), *b* is the kinetic fractionation that occurs during the fixation of CO₂ by ribulose-1,5 bisphosphate carboxylase-oxygenase (Rubisco) (27‰), and *p_i/p_a* is the ratio of the partial pressures of CO₂ in the substomatal cavity and the atmosphere, respectively.

Eqn. 1 indicates a positive linear relationship between Δ¹³C and *p_i/p_a*. The latter term (*C_{st}/C_a*) can be regarded as the set point for photosynthetic gas exchange reflecting overall trade-offs between carbon gain and water loss and associated characteristics that contribute to having a higher or lower rate of gas exchange activity. Plant carbon gain is linked directly to the operation of Rubisco, which catalyzes the rival processes of carboxylation (leading to photosynthesis) and oxygenation (leading to photorespiration). Both CO₂ and O₂ compete for the

* Author to whom correspondence should be addressed (d.j.beerling@sheffield.ac.uk).

first acceptor molecule ribulose biphosphate at their binding sites on Rubisco. Thus, CO₂ and O₂ are mutually competitive inhibitors (Lawlor, 1993). A rise in CO₂ competitively inhibits the oxygenase reaction of Rubisco, leading to the suppression of photorespiration, whereas a rise in O₂ tends to inhibit the carboxylation reaction, suppressing photosynthesis. The extent of O₂ inhibition of photosynthesis becomes diminished as atmospheric *p*CO₂ increases.

The unusually high O₂ and low CO₂ levels calculated for the Permo-Carboniferous (Berner and Canfield, 1989; Berner et al., 2000; Berner 2001; Berner and Kothavala, 2001) are predicted to have substantially shifted the balance of Rubisco operation in favor of the oxygenation reaction (Sage, 1999). Consequently, because of the lower photosynthetic draw-down of CO₂ in the substomatal cavity, the *p_i/p_a* ratio of nonstressed plants and Δ¹³C should have increased (Farquhar and Wong, 1984). This theoretical expectation has been verified by experiments with vascular plants grown in an O₂-enriched atmosphere (Berner et al., 2000). Besides this effect, an atmosphere with high O₂ can also lead to re-fixation of the increased flux of ¹³C-depleted (photo)respired CO₂ (Farquhar et al., 1982; Gillon et al., 1998) and increase the openness of stomatal pores (e.g., Rachmilevitch et al., 1999). Both of these additional O₂ influences on plant physiology operate to amplify any increase in Δ¹³C resulting from higher *p_i/p_a* ratios.

Against this background, therefore, we hypothesize that a major atmospheric O₂ pulse during the Permo-Carboniferous imprinted a detectable signature on the isotopic composition of fossil plant carbon. To test this hypothesis, we describe results from plant growth experiments with different O₂/CO₂ atmospheric mixing ratios and an extensive series of isotopic measurements on fossil plants. The experiments extend the range of species considered previously (Berner et al., 2000) and investigate the extent to which high O₂-related isotopic fractionation effects might be modified by the background atmospheric CO₂ level. In a separate experiment, we also examined if O₂ effects on Δ¹³C were reversible by growing plants in an atmosphere with a low (15%) O₂ level.

Following these experiments, we sought evidence for an O₂-related impact on plant carbon isotope fractionation in the fossil record by measuring the carbon isotope composition of well-preserved compression and permineralized plant fossils representing four major clades of land plants (the lycopsids; the trimerophytes, which lie basal to all land plants above the lycopsids; the filicopsids/sphenopsids; and the spermatophytes or seed plants). The measurements were made on fossil plants ranging in age from the Paleozoic to the mid-Cenozoic. Three clades (lycopsids, trimerophytes, and filicopsids/sphenopsids) were composed of free-sporing plants that first appeared in the Devonian. The fourth clade (spermatophytes) represents the seed-plant lineage, whose first species were Devonian members of the progymnosperms, a group ancestral to seed plants. Investigating a range of plant clades allowed us to search for Late Paleozoic high O₂ signature on species occupying different habitats and with likely different photosynthetic physiologies.

2. MATERIALS AND METHODS

2.1. Controlled Environment Plant Growth Experiments

Before the experiments, seeds of the herbaceous species *Phaseolus vulgaris* and *Sinapis alba* were germinated and cultivated at 25°C and

70% relative humidity with an irradiance of 250 μmol m⁻² s⁻¹ for 1 week. Seedlings were then transferred to controlled growth chambers with the same design and environmental regulation as given previously (Beerling et al., 1998), namely, four replicate chambers per species and per treatment. All experiments were conducted under a diurnal cycle of 14 h light and 10 h darkness and an irradiance of 250 μmol m⁻² s⁻¹. Plants were watered daily with 40 mL of dilute Rorison's solution. Each species was grown for 2 weeks in an atmosphere with the following atmospheric O₂ and CO₂ values:

- Experiment 1: high O₂, subambient CO₂ (treatment O₂ = 35%, CO₂ = 0.030%, control O₂ = 21%, CO₂ = 0.036%).
- Experiment 2: high O₂, elevated CO₂ (treatment O₂ = 35%, CO₂ = 0.045%, control O₂ = 21%, CO₂ = 0.036%).

In an additional experiment, we grew *P. vulgaris* under the following conditions:

- Experiment 3: low O₂, ambient CO₂ (treatment O₂ = 15%, CO₂ = 0.035%, control O₂ = 21%, CO₂ = 0.036%).
- The background levels of CO₂ were selected to represent those derived from sensitivity analyses using a long-term geochemical model of the carbon cycle (Berner and Kothavala, 2001).
- In all experiments, the nighttime temperature was 20 ± 2°C. Daytime temperature (*t_d*) and water vapor pressure deficit (VPD) of the air varied between experiments but not between treated and control chambers for any given experiment: experiment 1, *t_d* = 25 ± 2°C, VPD = 1.2 to 1.6 kPa; experiment 2, *t_d* = 28 ± 2°C, VPD = 1.4 to 1.8 kPa; experiment 3, *t_d* = 32 ± 2°C, VPD = 1.8 to 2.4 kPa. The increase in Δ¹³C values of the control *P. vulgaris* plants (Tables 2 and 3) resulted from a slight upward drift in the growth temperature of the experiments (see above). This effect does not compromise our results because it is the opposite to that shown by fossil plant Δ¹³C, which increased between the Devonian and the Carboniferous, while the climate cooled.

2.2. Carbon Isotope Analyses

For the laboratory experiments, mature whole leaves that had fully developed under the experimental treatment were harvested, dried for 1 week at 40°C, and powdered. Samples were combusted to CO₂ and analyzed in triplicate at the Biomedical Mass Spectrometry Unit, University of Newcastle, UK. Gas samples of the mixtures exiting each individual chamber were collected at six regular intervals during each run, and CO₂ was isolated. For comparison, gas mixtures entering the chambers were also sampled at the start of each experiment. The isotopic composition of CO₂ entering and exiting the chambers typically differed by <2‰, and the means of all measurements were used.

Fossil plant carbon was collected from the specimens listed in Table 1. In most cases, samples selected for carbon isotope analyses were securely identified, well dated, with provenance data, and possessed intact carbon structure. All samples were handled with forceps, powdered, and their isotopic ratios measured by combustion at Indiana University or Yale University.

Carbon isotopic composition (δ¹³C) is expressed as [*R*_{(sample)/*R*_(standard)} - 1] × 1000, where *R* is the ¹³C/¹²C ratio of each sample and the Pee Dee Belemnite standard. Plant Δ¹³C was calculated according to (Farquhar et al., 1982):

$$\Delta^{13}\text{C} = \frac{(\delta^{13}\text{C}_a - \delta^{13}\text{C}_p)}{\left(1 + \frac{\delta^{13}\text{C}_p}{1000}\right)}, \quad (2)$$

where δ¹³C_a and δ¹³C_p are the isotopic compositions of atmospheric CO₂ and the plants, respectively. Operational *p_i/p_a* ratios, corresponding to Δ¹³C values, were calculated after rearrangement of Eqn. 1.

For the fossil plants, Δ¹³C was calculated using the isotopic composition of atmospheric CO₂ estimated from a smoothed curve fitted to the extensive compilation of isotopic measurements on carefully selected Paleozoic and mid-Cenozoic marine calcium carbonate fossils (Veizer et al., 1999). This approach assumes the regulation of δ¹³C_a on a long-term basis by equilibrium with marine inorganic carbon. All δ¹³C_a values were calculated as being 7‰ more negative than the carbonate record to account for the difference between seawater and the

Table 1. Carbon isotope composition of plant fossils ($\delta^{13}C_p$) and of atmospheric CO₂ ($\delta^{13}C_a$). Values of isotope discrimination ($\Delta^{13}C$) calculated via Eqn. 2.

Lineage	Specimen number ^a	Geologic epoch	Age (Myr) ^b	Location	Material analyzed	Preservation	$\delta^{13}C_p$ (‰) ^c	$\delta^{13}C_a$ (‰)	$\Delta^{13}C$ (‰)
Fossils									
Trimerophyte clade									
<i>Psilophyton forbesii</i>	10118	Early Devonian	388 ± 2	New Brunswick, Can	Axes	Compression	-25.4	-6.0	19.9
<i>P. forbesii</i>	20014	Early Devonian	388 ± 2	Gaspé, Quebec, Can	Axes	Compression	-26.3	-6.0	20.8
Lycopodiid clade									
<i>Leclercqia complexa</i>	452 (n = 3)	Middle Devonian	378 ± 2	Schoharie Co., NY	Leaves and axes	Compression	-21.3 ± 0.09	-6.0	15.6
<i>Lepidodendropsis vander</i>	5968	Early Mississippian	342 ± 11	Palauski, WV	Sporophylls	Compression	-23.5	-3.3	20.7
<i>Lepidostrobos variabilis</i>	23492	Early Pennsylvanian	319 ± 4	Pottsville, PA	Sporophylls	Compression	-24.3	-2.5	22.3
<i>Stigmaria ficooides</i>	23220	Early Pennsylvanian	315 ± 8	Ottsville, PA	Root	Compression	-23.1	-2.3	21.3
Filicopsid/sphenopsid clade									
<i>Rhacophyton ceratantianum</i>	470	Late Devonian	365 ± 3	Valley Head, WV	Axes	Compression	-24.0	-5.3	19.2
<i>Sphenophyllum emarginatum</i>	7592b	Early Pennsylvanian	311 ± 1	St. Clair, PA	Leaves and axes	Compression	-24.1	-2.2	22.4
<i>Rhacopteris elegans</i>	35401	Middle Pennsylvanian	308 ± 1	Stradonitz, Czech Europe	Leaf rachis	Permineralized	-22.3	-2.1	20.7
<i>Pecopteris plumosa-dentata</i>	35806	Middle Pennsylvanian	304 ± 14		Leaves and rachises	Compression	-24.2	-2.1	22.6
Calamites pachydermis									
<i>Psaronius infarctus</i>	40030	Late Pennsylvanian	301 ± 11	Waldenburg, Silesia	Axis	Compression	-23.8	-2.0	22.3
<i>Cladophlebis</i> sp. (n = 2)	35832	Early Permian	277 ± 13	Chemnitz, Germany	Axis	Permineralized	-24.9	-2.4	23.1
<i>Cladophlebis denticulata</i>	45148	Middle Jurassic	170 ± 1	Cayton Bay, England	Leaves	Compression	-23.7 ± 0.9	-5.6	18.5
<i>Fern</i> spp.	45149	Middle Jurassic	170 ± 1	Cayton Bay, England	Leaves	Compression	-21.3	-5.6	16.0
	45150	Middle Jurassic	169 ± 1	Cayton Bay, England	Leaves	Compression	-24.5	-5.6	19.4
Spermatophyte clade									
<i>Eospermatopteris erianus</i>	7008e	Mid-Devonian	377 ± 1	Gilboa, NY	Axes	Compression	-24.4	-5.8	19.1
<i>Archaeopteris jacksonii</i>	36888/50503 (n = 2)	Late Devonian	372 ± 2	Escuminac, Quebec, Can.	Leaves and axes	Compression	-28.1 ± 0.5	-5.1	23.7
A. macilenta									
<i>Triphylopteris uberis</i>	36886	Late Devonian	366 ± 1	Hancock, NY	Leaves and axes	Compression	-25.4	-5.1	20.8
<i>Glossopteris borassifolius</i>	943	Early Mississippian	347 ± 7	Pulaski Co., WV	Axes	Compression	-23.5	-3.3	20.7
<i>Trigonocarpon</i> sp.	35370	Middle Pennsylvanian	309 ± 2	Cannelton, PA	Leaf	Compression	-23.8	-2.2	22.0
<i>Walchia piniformis</i>	7598b (n = 3)	Middle Pennsylvanian	305 ± 0.5	St. Clair, PA	Seed	Compression	-23.6 ± 0.3	-2.1	22.0
<i>Alethopteris</i> sp.	24977 (n = 2)	Late Pennsylvanian	304 ± 14	Berschweiler, Ger.	Axes	Compression	-24.8 ± 0.05	-2.1	23.3
<i>Medullosa stellata</i>	30069	Late Pennsylvanian	295 ± 1	Lawrence, KS	Leaves	Compression	-25.0	-2.0	23.6
<i>Glossopteris amplia</i>	6014	Early Permian	277 ± 13	Hilbersdorf, Ger.	Axis	Permineralized	-27.0	-2.3	25.4
<i>Walchia sternbergii</i>	26178	Late Permian	255 ± 2	Newcastle, NSW, Aust.	Leaves and axes	Compression	-24.7	-3.5	21.7
<i>Ullmania bromii</i>	12703	Late Permian	253 ± 3	Lodeve, France	Leaves and axes	Compression	-23.6	-3.7	20.4
<i>Philophyllum</i> sp.	27836 (n = 2)	Late Permian	253 ± 3	Gera, Saxony, Ger.	Fruit	Compression	-25.2 ± 0.1	-3.7	22.1
<i>Otozamites hespera</i>	4829	Late Triassic	227 ± 2	Leaksville, VA	Leaf	Compression	-22.4	-5.3	19.6
<i>Czekanowskia rigida</i>	4906	Late Triassic	227 ± 2	Gulf, NC	Leaves	Compression	-22.9	-5.3	18.0
<i>Pachypteris</i> sp.	25826	Early Jurassic	206 ± 2	Stabbarp, Sweden	Leaves	Compression	-23.9	-6.1	18.2
	45151	Middle Jurassic	176 ± 2	Yorkshire, England	Leaves	Compression	-24.8	-5.7	19.6

(continued)

62
63
64
65
66
67
68
69
70
71
72
73
74
75
76
77
78
79
80
81
82
83
84
85
86
87
88
89
90
91
92
93
94
95
96
97
98
99
100
101
102
103
104
105
106
107
108
109
110
111
112
113
114
115

Table 1. (Continued)

Lineage	Specimen number ^a	Geologic epoch	Age (Myr) ^b	Location	Material analyzed	Preservation	$\delta^{13}C_p$ (‰) ^c	$\delta^{13}C_a$ (‰)	$\Delta^{13}C$ (‰)
<i>Nilssonia</i> sp.	45152	Middle Jurassic	170 ± 1	Cayton Bay, England	Leaves	Compression	-25.4	-5.6	20.3
<i>Ginkgo huttonii</i> (n = 2)	45153/4 (n = 2)	Middle Jurassic	170 ± 2	Scalby Ness, England	Leaves	Compression	-25.9 ± 0.5	-5.6	20.8
<i>Otozamites ribetiroanus</i>	36203	Middle Jurassic	159 ± 2	Portugal	Leaves	Compression	-22.6	-5.5	17.5
<i>Dioonites buchianus</i>	45157	Early Cretaceous	123 ± 3	Richmond, VA	Leaves	Compression	-20.5	-4.7	16.1
<i>D. buchianus</i>	48915/6 (n = 2)	Early Cretaceous	123 ± 3	Richmond, VA	Leaves	Compression	-22.6 ± 0.05	-4.7	18.3
Conifer wood (unid.)	45155	Early Cretaceous	118 ± 6	College Park, MD	Wood	Compression	-20.9	-4.5	16.8
Conifer wood (unid.)	45156	Early Cretaceous	118 ± 6	College Park, MD	Wood	Compression	-22.8	-4.5	18.7
" <i>Sapindus</i> " <i>morrisonii</i>	5848	Late Cretaceous	94 ± 3	Arthurs Ferry, TX	Leaves	Compression	-26.5	-4.5	22.6
<i>Laurophyllum angustifolium</i>	22556	Late Cretaceous	87 ± 1	Cliffwood Beach, NJ	Leaves	Compression	-25.5	-4.5	21.6
<i>Androvetitia carolinensis</i>	50501/2 (n = 2)	Late Cretaceous	79 ± 3	Neuse River, NC	Leaves and axes	Compression	-25.0 ± 0.05	-4.6	20.9
Modern plants ^d									
Seed plants		Present day	0		Leaves	Fresh	-28.8 ± 2	-8.0	21.4

^a All specimens have the prefix YPM and are deposited in the Peabody Museum of Natural History, Yale University. Locality details may be secured from www.peabody.yale.edu. Where appropriate, replication = of measurement (n) made on the same fossil is also given.

^b Estimated from the original literatures sources (L. J. Hickey, unpublished data).

^c For replicate analyses made on the same fossil, the mean ± s.e. term is given.

^d Data for the extant seed plants (trees and herbs) from measurements Körner et al. (1988) (n = 61 species), errors indicate ± 1 s.e., and the $\delta^{13}C_a$ value from Keeling et al. (1995).

Table 2. Carbon isotope composition of vascular plants ($\delta^{13}C_p$) and of atmospheric CO₂ ($\delta^{13}C_a$) as measured in plant growth experiments at different O₂ levels. Measurement errors in ± s.e. Mean ratio of substomatal cavity to atmospheric CO₂ (p_i/p_a), and water-use efficiency (WUE) derived as described in the text. Values in bold type indicate growth CO₂ levels, values in parentheses the O₂/CO₂ mixing ratio.

Species	$\delta^{13}C_p$ (‰)	$\delta^{13}C_a$ (‰)	$\Delta^{13}C$ (‰)	p_i/p_a (unitless)	WUE (mmol CO ₂ /mol H ₂ O)	Growth O ₂ concentration		$\Delta^{13}C$ (‰)	$\Delta(\Delta^{13}C)^a$ (‰)
						21% O ₂	35% O ₂		
<i>Phaseolus vulgaris</i>	-25.7 ± 0.4	-7.8 ± 0.9	18.3	0.62	86.6	-28.7 ± 0.6	0.030% CO₂ (1167)	21.0	+3.4
	-28.1 ± 0.4	-7.1 ± 0.5	21.6	0.76	53.8	-31.9 ± 0.2	-8.3 ± 1.2 -9.3 ± 0.4	23.3	+1.7
<i>Ranunculus repens</i> ^b	-23.0 ± 0.6	-3.2 ± 0.7	20.3	0.70	61.1	-26.7 ± 0.3	0.033% CO₂ (1060)	21.8	+1.5
	-22.3 ± 0.2	-4.5 ± 0.9	18.2	0.61	81.3	-27.0 ± 1.1	-5.5 ± 0.8 -6.0 ± 0.9	21.6	+3.4
<i>Macrozamia communis</i> ^b	-26.2 ± 0.5	-7.3 ± 1.8	19.4	0.66	75.7	-34.8 ± 0.6	0.045% CO₂ (777)	20.7	+1.3
	-24.2 ± 0.5	-7.3 ± 0.4	17.3	0.57	96.6	-37.2 ± 0.2	-14.8 ± 0.7 -17.1 ± 0.3	20.7	+3.4

^a Calculated as $\Delta(\Delta^{13}C) = \Delta^{13}C$ (at experimentally altered O₂ value) - $\Delta^{13}C$ (at 21 % O₂) = change in fractionation from control conditions.

^b Recalculated using Eqn. 2 from the data reported by Berner et al. (2000).

ards, 1984). A simplified relationship between plant WUE and p_i/p_a is given by (Farquhar and Richards, 1984):

$$\text{WUE} = \frac{A}{g_s} = \frac{P_a \times \left(1 - \frac{p_i}{p_a}\right)}{1.6}, \quad (3)$$

where 1.6 accounts for the difference in the gases diffusivities of CO_2 and water vapor in air.

Eqn. 3 allows a first quantification of the effects of growth under the different atmospheric O_2/CO_2 mixing ratios on plant WUE (Tables 2 and 3). Calculated from Eqn. 3, leaf WUE of all of the species so far examined decreased with an increase in atmospheric O_2 when background atmospheric CO_2 levels were $\leq 0.033\%$ (Table 2). The opposite case was observed for the subambient O_2 trials (Table 3). Clear species-specific differences are apparent in these responses relating to mesophyll carboxylation capacity and stomatal responses to the environment. The mean WUE response of *P. vulgaris* and *S. alba* to growth in an O_2 atmosphere enriched to 35% with $\text{CO}_2 = 0.030\%$ was a reduction of 40% compared to the control (Table 2). However, when O_2 is enriched to 35% with $\text{CO}_2 = 0.045\%$, the reduction in WUE is diminished, falling by only 7% relative to the control. These WUE responses, derived experimentally, support results from completely independent simulations of the effects of different atmospheric O_2/CO_2 mixing ratios on the annual productivity and transpiration of vegetation simulated at the global scale under a Late Carboniferous climate using a process-based terrestrial carbon cycle model (Beerling and Berner, 2000).

In summary, our experiments (Table 2), together with earlier observations (Berner et al., 2000), establish that if atmospheric O_2 levels rose to 35% during the Permo-Carboniferous, it is likely to have increased the isotopic fractionation between land plant carbon and atmospheric CO_2 with the potential to imprint a detectable signature in the isotope composition of fossil plants. This effect would be apparent even if background atmospheric CO_2 levels were ~ 450 ppm (Table 2).

3.2. Carbon Isotope Fractionation Patterns in Fossil Plants

The LOESS curve fitted to the time series of $\delta^{13}\text{C}_p$ measurements on our fossil plant specimens depicts weakly defined oscillations between the Devonian and the late Mesozoic (Fig. 1). Eqn. 1 and 2 indicate that this pattern includes the physiologic responses of plants to global changes in the environment and to the effects of changes in the isotopic composition of atmospheric CO_2 , $\delta^{13}\text{C}_a$. Variations in $\delta^{13}\text{C}_a$ can be deduced from the smoothed marine carbonate curve of Veizer et al. (1999), assuming equilibrium between the two reservoirs. The carbonate record shows a distinct excursion toward more positive values during the Permo-Carboniferous period (Berner, 2001), partly because terrestrially derived plant debris (which is isotopically more negative than carbonates) was a major source of buried organic matter at this time. We removed the effect of $\delta^{13}\text{C}_a$ by calculating plant carbon isotope fractionation ($\Delta^{13}\text{C}$) during growth (Eqn. 2, Fig. 1). The resulting pattern shows a much clearer trend, with $\Delta^{13}\text{C}$ values rising and falling over the Permo-Carboniferous interval (Fig. 1). A further rise in plant

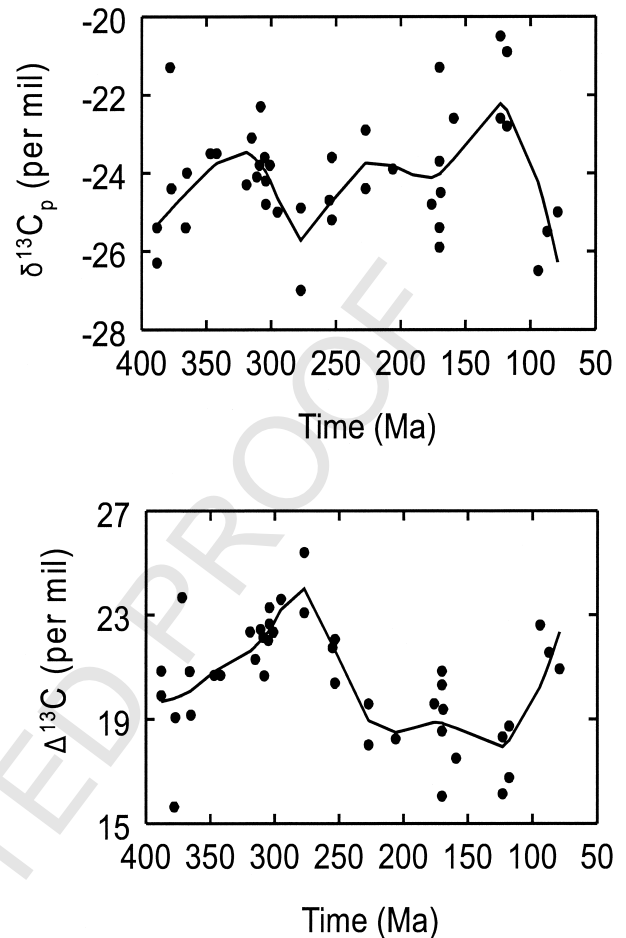


Fig. 1. Changes in fossil plant isotope composition ($\delta^{13}\text{C}_p$) (upper panel) and reconstructed changes in ^{13}C discrimination ($\Delta^{13}\text{C}$), calculated from Eqn. 2 using the marine carbonate record to estimate isotopic composition of atmospheric CO_2 ($\delta^{13}\text{C}_a$) (lower panel). The solid lines in both cases depict the locally weighted least squares regression curves (LOESS, $\text{span} = 0.4$) fitted to the data.

$\Delta^{13}\text{C}$ between 125 Ma and the present is also apparent. The clear Late Paleozoic $\Delta^{13}\text{C}$ excursion indicates that fossil plants exhibit an isotopic signal that may be due to variations in atmospheric O_2 .

It emerges that a comparison between plant $\Delta^{13}\text{C}$ values and modeled O_2 variations predicted using both sediment abundance (Berner and Canfield, 1989) and carbon and sulfur isotope mass balance (Garrels and Lerman, 1984; Berner et al., 2000; Berner, 2001) models shows reasonable agreement (Fig. 2). In particular, the rise and fall in plant $\Delta^{13}\text{C}$ values broadly corresponds to the predicted rise and fall in atmospheric $p\text{O}_2$ and reflects changes in their operational p_i/p_a ratios (Fig. 2). This agreement at first sight might appear to be tautological because of the use of the carbon isotopic data for carbonates in both the isotope mass balance modeling and the determination of $\Delta^{13}\text{C}$. If there had been a parallelism between the fossil organic carbon $\delta^{13}\text{C}_p$ record and the carbonate $\delta^{13}\text{C}$ record, this would have implied no change in $\Delta^{13}\text{C}$. However, this was not found. The plant $\delta^{13}\text{C}$ values do not track the carbonate $\delta^{13}\text{C}$ values, meaning that $\Delta^{13}\text{C}$ must have changed with time.

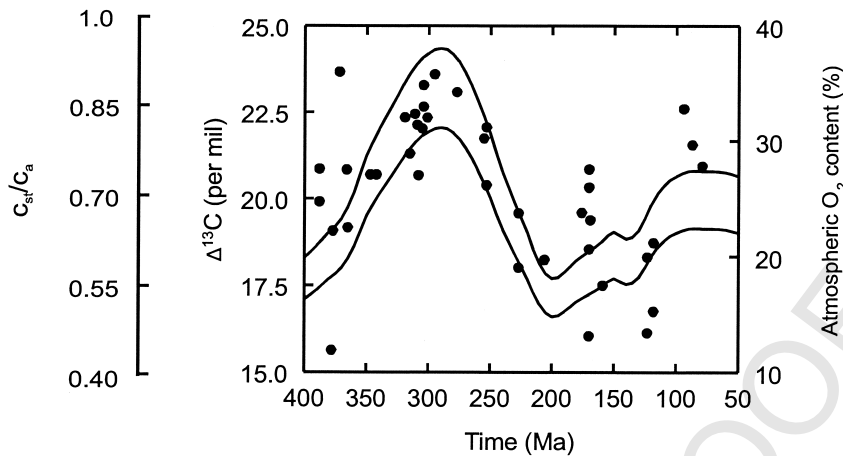


Fig. 2. Comparison of changes in fossil plant $\Delta^{13}\text{C}$ values (Fig. 1) (●) and calculated changes in the atmospheric O₂ content (solid lines) (Berner et al., 2000; Berner, 2001) during the Late Paleozoic. The upper and lower solid lines indicate a measure of the uncertainty in predicted atmospheric O₂ content based on model sensitivity analyses (Berner, 2001). The left-hand axis also shows changes in the ratio of the partial pressures of CO₂ in the substomatal cavity and the atmosphere (p_i/p_a ratio) corresponding to the $\Delta^{13}\text{C}$ values calculated from Eqn. 1.

Further, the results of Berner and Canfield (1989) for O₂ are not based on isotopic data.

The direction of $\Delta^{13}\text{C}$ changes as modeled O₂ increased and then decreased is consistent with photosynthetic theory of O₂ effects on land plants (Farquhar and Wong, 1984) and our experimental observations (Table 2) (Berner et al., 2000). Bocherens et al. (1994) reported an extensive set of isotopic measurements on fossil plants between the Triassic and the Early Tertiary. Combining that data set with estimates of $\delta^{13}\text{C}_a$ reveals a fall in plant $\Delta^{13}\text{C}$ of 4‰ between the Triassic and the Middle Jurassic, in agreement with our measurements. It also, however, suggests a continued decline in fossil $\Delta^{13}\text{C}$ in the Late Cretaceous, which is at odds with our predictions and observations (Fig. 2). Overall, given that fossil plant isotope records and O₂ predictions are independent of each other, we suggest that the agreement in direction and timing of $\Delta^{13}\text{C}$ variations lends support to a modeled O₂ pulse during the Late Paleozoic.

We recognize that several environmental variables (e.g., precipitation, atmospheric moisture, temperature) other than O₂ might potentially influence plant $\Delta^{13}\text{C}$ (Farquhar et al., 1989) and cannot exclude their effects on the fossil plant $\Delta^{13}\text{C}$ record (Fig. 1). One such influence was seen in our analysis of the mid-Silurian bryophytic *Nematothallus* from the Bloomsburg Formation of Pennsylvania, which because of its growth habit as a thallus mat in direct contact with the soil surface gave light values (-27.1‰) that could have been due to the incorporation of ¹³C-depleted soil CO₂ during photosynthesis. This result was thus excluded from our data set. However, the lycopsids, filicopsids, and sphenosids all possessed water-conducting systems of limited efficiency, restricting their distribution to humid, moist habitats with an adequate supply of soil water. Isotopic analysis of these clades therefore allowed us to control for the effects of Late Paleozoic environmental change and assess only the impact of atmospheric composition during growth on $\Delta^{13}\text{C}$. Summarizing the data in Table 1 for the lycopsids and filicopsids/sphenosids indicates consistent $\Delta^{13}\text{C}$ increases between the Devonian and the Carboniferous (Fig. 3).

For these groups, we suggest that Late Paleozoic climate change by itself was unlikely to be responsible for the observed shifts in $\Delta^{13}\text{C}$. The spermatophytes, occupying more variable habitats, also exhibit marked $\Delta^{13}\text{C}$ increases between the Devonian and the Carboniferous, but with between-sample differences for the Devonian specimens (Table 1, Fig. 3). Over a longer time scale, the Mesozoic samples of fossil plant specimens of the ferns and their allies (filicopsids and sphenosids) and the spermatophytes confirm that their operational $\Delta^{13}\text{C}$ was unusually high during the Late Paleozoic relative to the Mesozoic situation, when values were lower by ~4‰ (Fig. 3). Indeed, a global survey of carbon isotope discrimination by modern floras distributed between the polar and equatorial regions revealed that plants with characteristic $\Delta^{13}\text{C}$ values > 22‰ are comparatively infrequent (Körner et al., 1991), in agreement with global model estimates of the extent of discrimination against ¹³C during the growing season based on stomatal responses to the environment (Lloyd and Farquhar, 1994).

Averaging for each geologic period across all the four clades gives a $\Delta^{13}\text{C}$ rise of ~5.0‰ between the Devonian and the close of the Permian (Fig. 3). The increase is of a similar magnitude to that reported for a less-detailed independent set of isotopic measurements on coals from the UK (Jones, 1994), which showed a 4.6‰ increase in $\Delta^{13}\text{C}$ between the Lower and Upper Carboniferous. It is also in agreement with the data of Mora et al. (1996), who reported an increase of 2.1‰ in the discrimination between the isotopic composition of bulk soil organic matter and atmospheric CO₂ between 410 and 282 Ma. Both are somewhat larger than recorded by fossil plants in response to the last glacial-interglacial cycle of environmental change (Van der Water et al., 1994; Turney et al., 1997).

Atmospheric $p\text{CO}_2$ is a potentially important consideration influencing fossil plant $\Delta^{13}\text{C}$ patterns, since the Permo-Carboniferous was associated with a marked draw-down due to enhanced silicate rock weathering and organic carbon burial (Mora et al., 1996; Berner and Kothavala, 2001). Mechanistically based leaf gas exchange simulations (Beerling, 1996) and

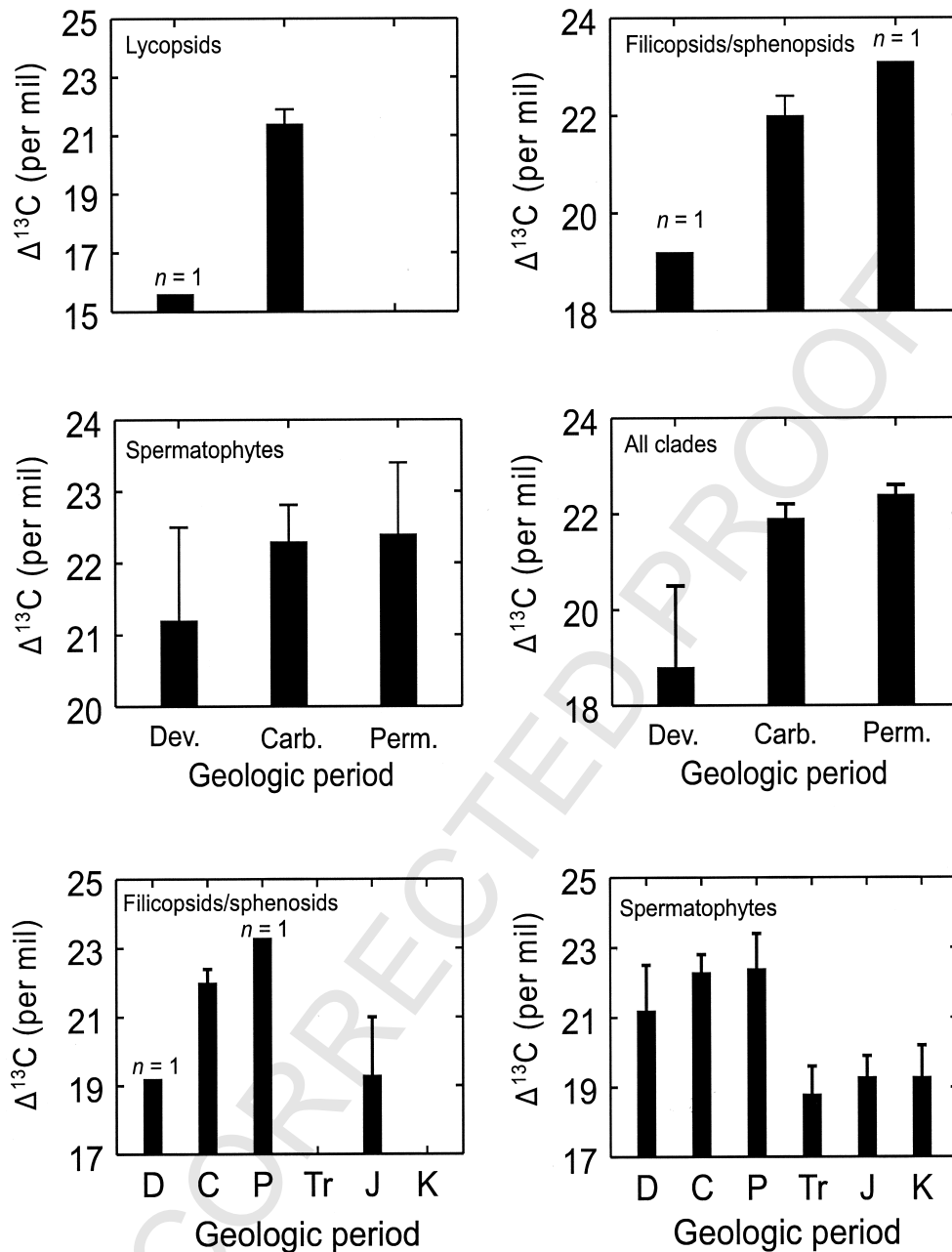


Fig. 3. Mean (\pm s.e.) plant $\Delta^{13}\text{C}$ as a function of geologic period for various clades between the Devonian and the Permian (calculated from data in Table 1). Also illustrated are mean trends in $\Delta^{13}\text{C}$ for two clades between the Devonian and the Cretaceous.

experimental data indicate that the carbon isotopic composition of plants exhibits a very low sensitivity to CO_2 change over the range 0.02 to 0.07% (Arens et al., 2000). However, more data on the effect of widely varying atmospheric CO_2 concentrations but at a constant O_2 level are needed to further test this conclusion.

Our new extensive fossil plant $\Delta^{13}\text{C}$ data set (Table 1) has been used to test a function describing the dependence of carbon isotope fractionation between carbonates and organic matter (due to photosynthesis) on atmospheric O_2 (Berner et al., 2000; Berner, 2001). The significance is that when used in

the isotope mass balance model of Garrels and Lerman (1984), O_2 -dependent changes in the ^{13}C fractionation between carbonates and organic matter result in an O_2 history bounded by less extreme and biologically acceptable levels (Berner et al., 2000). It is assumed in the modeling that the fractionation between CO_2 and carbonates and between original plants and their buried organic remains stays constant over time so that variations in the differences in $\delta^{13}\text{C}$ between carbonates and organic matter are due solely to photosynthesis. The function, derived from the results of a limited set of plant and plankton growth experiments with artificially altered O_2 environments (Berner

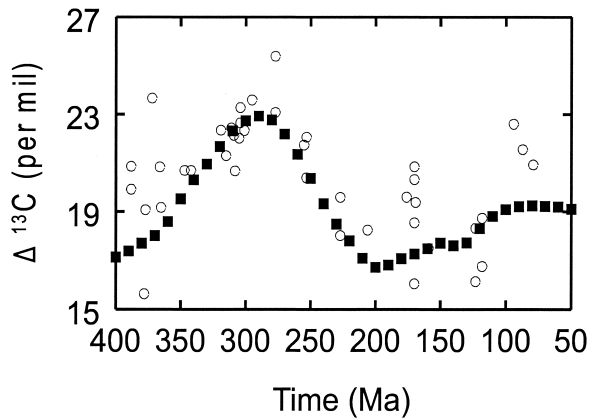


Fig. 4. Observed (○) and predicted (■) changes in Late Paleozoic plant $\Delta^{13}\text{C}$ values. Predicted values were calculated from Eqn. 4. See text for details.

et al., 2000), models the O₂ dependence of the fractionation between fossil organic matter and CO₂, $\Delta^{13}\text{C}_{\text{mod}}$, as:

$$\Delta^{13}\text{C}_{\text{mod}} = \Delta^{13}\text{C}_{\text{phot}} + J \times \left[\left(\frac{M_{\text{O}_2}}{38} \right) - 1 \right], \quad (4)$$

where $\Delta^{13}\text{C}_{\text{phot}}$ represents the present-day carbon isotope fractionation between atmospheric CO₂ and photosynthetically produced carbon (18.5‰ for the present level of O₂), J is an adjustable curve fit parameter, M_{O_2} is the mass of oxygen in the atmosphere, and 38 is the mass of oxygen in the present atmosphere (in 10¹⁸ mol). For this test, Eqn. 4 was used with $J = 5$ to predict $\Delta^{13}\text{C}_{\text{mod}}$ (Berner et al., 2000; Berner, 2001) for comparison with observed changes in fossil plant $\Delta^{13}\text{C}$. It emerges that Eqn. 4 predicts Phanerozoic variations in plant $\Delta^{13}\text{C}$ remarkably well, particularly during the Late Paleozoic (Fig. 4), indicating its likely general applicability and supporting its use in isotopic mass balance models of atmospheric O₂. That the positive excursion of isotopic fractionation during the Permo-Carboniferous is a general phenomenon and not confined only to plants is shown by the data of Hayes et al. (1999), who found a similar excursion for the difference between carbonate carbon and total organic carbon (which includes marine-derived material) in sedimentary rocks (Berner, 2001).

3.3. Calibration of Fossil Plant $\Delta^{13}\text{C}$ Determinations

The experimental data documenting the effects of plant growth in different O₂/CO₂ atmospheric mixing ratios on $\Delta^{13}\text{C}$ can be expressed as the change in carbon isotope fractionation (denoted here as $\Delta(\Delta^{13}\text{C})$) relative to fractionation for the controls at present-day conditions (21% O₂, 0.036% CO₂). Calculation of $\Delta(\Delta^{13}\text{C})$ for our new data sets and those reported by Berry et al. (1972) and Berner et al. (2000) yields a nonlinear relationship when plotted against the altered O₂/CO₂ ratio, within the range (140 to 1066) for which we have observations (Fig. 5). The relationship predicts that plant growth in an atmosphere with O₂ = 35% and CO₂ = 0.03% (i.e., an O₂/CO₂ ratio of 1166) increases isotopic fractionation relative to the contemporary situation to a greater extent than if

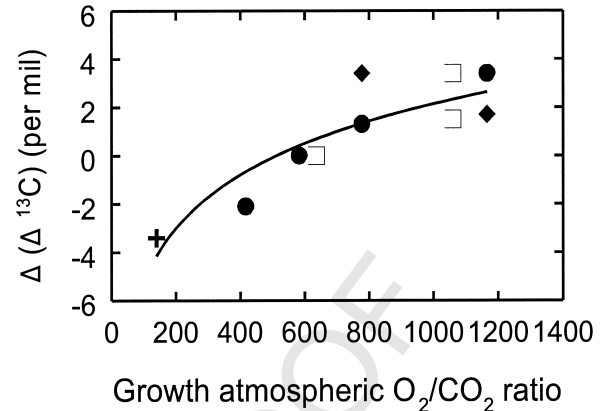


Fig. 5. Relationship between change in $\Delta(\Delta^{13}\text{C})$ of vascular land plants determined experimentally in response to growth under different O₂/CO₂ atmospheric mixing ratios. $\Delta(\Delta^{13}\text{C})$ is the change in carbon isotope fractionation relative to fractionation for the controls at present-day conditions (21% O₂, 0.036% CO₂). Codes: (●) *Phaseolus vulgaris*, (◆) *Sinapis alba*, (□) data from Berner et al. (2000), and (+) data from Berry et al. (1972). The solid line shows the nonlinear curve fitted to the data, given by $\Delta(\Delta^{13}\text{C}) = -19.94 + 3.195 \times \ln(\text{O}_2/\text{CO}_2 \text{ mixing ratio})$, $r^2 = 0.78$.

the same O₂ rise occurred with a CO₂ level of 0.05% (i.e., an O₂/CO₂ ratio of 700) (+3 vs. +1‰).

To investigate the potential of Fig. 5 for extracting quantitative information on the composition of the paleoatmosphere from the fossils, we applied it as preliminary calibration function to predict past O₂/CO₂ ratios from fossil plant $\Delta^{13}\text{C}$. Ancient atmospheric O₂/CO₂ mixing ratios were calculated by inverse regression (Draper and Smith, 1983) of the equation describing the curve, giving:

$$\frac{\text{O}_2}{\text{CO}_2} = \exp[0.3189 \times (\Delta^{13}\text{C}_{\text{fossil}} - \Delta^{13}\text{C}_{\text{extnt}}) + 6.24], \quad (5)$$

where the term $(\Delta^{13}\text{C}_{\text{fossil}} - \Delta^{13}\text{C}_{\text{extnt}})$ is equivalent to $\Delta(\Delta^{13}\text{C})$ in Fig. 5, and $\Delta^{13}\text{C}_{\text{fossil}}$ and $\Delta^{13}\text{C}_{\text{extnt}}$ are the discriminations of the fossil and extant modern plants, respectively. The value of $\Delta^{13}\text{C}_{\text{extnt}}$ was taken from a global survey of $\delta^{13}\text{C}_\text{p}$ measurements made on low-altitude (0 to 900 m asl) modern herb and tree species ($n = 61$ species) and a $\delta^{13}\text{C}_\text{a}$ value of -8‰ (Keeling et al., 1995). No correction has been made in comparing fossil and living plant $\Delta^{13}\text{C}$ values because extensive measurements on bulk fossil carbon from leaves, flowers, seeds, and woods dating from the Triassic to the Late Tertiary suggest insignificant diagenetic alteration relative to modern values (Bocherens et al., 1994). In part, this is probably because differential decay of different plant compounds occurs quickly following the incorporation of the materials into the sedimentary record (Benner et al., 1987).

Application of Eqn. 5 to predict the past history of atmospheric O₂/CO₂ variations using plant fossils reveals a sharp Late Paleozoic increase and fall followed by rising values between 200 and 50 Ma (Fig. 6). The overall pattern of change reconstructed from fossils is generally consistent with the O₂/CO₂ ratio calculated from $p\text{O}_2$ predictions from a carbon and

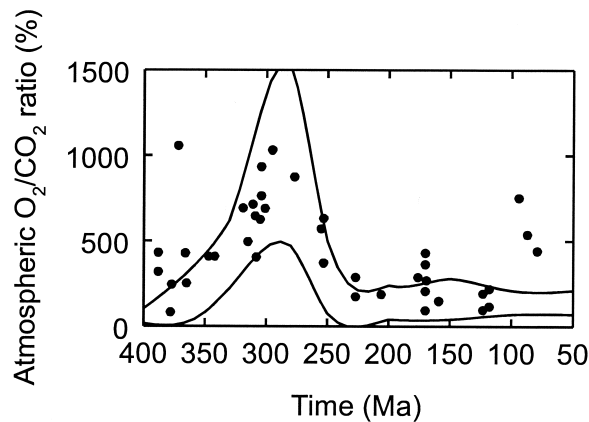


Fig. 6. Reconstructed variations in the atmospheric O_2/CO_2 mixing ratio using fossil $\Delta^{13}C$ values and the experimentally derived calibration function (\bullet) (Fig. 5, Eqn. 5). The continuous lines indicate the variation in pO_2/pCO_2 mixing ratios calculated from long-term models of the global carbon (Berner and Kothavala, 2001) and oxygen cycle (Berner et al., 2000; Berner, 2001). Upper and lower lines denote the envelope of uncertainty in the model predictions calculated from sensitivity analyses with both models.

sulfur isotopic mass balance model (Berner et al., 2000; Berner, 2001) combined with CO_2 predictions of a model of the long-term carbon cycle (Berner and Kothavala, 2001) (Fig. 6). Although the comparison is quite promising, further growth experiments on vascular land plants of different lineages (e.g., more ancient taxa such as ferns, cycads, and ginkgoales) under a much wider range of CO_2 levels at constant O_2 are required to narrow uncertainties in reconstructing the composition of the ancient atmosphere using the isotopic approach described here.

4. CONCLUSION

We have attempted to integrate plant physiologic processes with fossil plant isotope geochemistry to develop and interpret a time series of fossil plant $\Delta^{13}C$, derived from analysis of specimens constituting several different clades. The experimental data establish that plant growth in an O_2 atmosphere enriched to 35% increases carbon isotope fractionation but to an extent dependent upon the atmospheric O_2/CO_2 mixing ratios. Reconstruction of changes in plant $\Delta^{13}C$ using fossil plant $\delta^{13}C_p$ measurements and an estimate of $\delta^{13}C_a$ of atmospheric CO_2 based on the marine carbonate record yields a pattern of change during the Permo-Carboniferous consistent with the experimental results for the effect of a rise in O_2 on plants. Further, the excursion in fossil plant $\Delta^{13}C$ values during the Late Paleozoic mirrors the trajectory of O_2 change predicted from long-term sediment abundance and carbon and sulfur isotope mass balance models. Indeed, a preliminary calibration of the $\Delta^{13}C$ record to predict changes in the O_2/CO_2 mixing ratio of the ancient atmosphere supports to a limited extent the combined O_2/CO_2 reconstructions from long-term models of the global carbon and oxygen cycles.

The experimental and fossil data provide the strongest evidence yet that Earth experienced a major O_2 pulse during the Late Paleozoic, strengthening its hypothesized role in the diversification and ecological radiation of the Late Paleozoic

fauna and flora (Robinson, 1989; Graham et al., 1995). A high O_2 content in the Permo-Carboniferous could have increased stratospheric ozone production, thus providing better shielding against ultraviolet radiation for surface ocean and terrestrial organisms. In addition, an O_2 -driven decrease in WUE of vegetation could alter the exchange of energy and materials between the land surface and the atmosphere with a feedback on regional and global climate, a feature not yet considered in paleoclimate modeling studies of the Carboniferous or Permian (Otto-Bliesner, 1993; Beerling, et al., 1998; Valdes and Crowley, 1998; Rees et al., 1999). Critically, our data call for the urgent need to better understand the role of O_2 in the ignition and spread of forest fires in the Carboniferous (Watson et al., 1978; Robinson, 1989; Lenton and Watson, 2000).

Acknowledgments—We thank G. D. Farquhar, J. Gillon, and F. I. Woodward for comments and discussion and Gillion Taylor and Rick Dunn for careful calibration of the isotopic samples from the experiments. Assistance in preparing fossil samples for isotopic analysis at Yale was provided by W. Green. D. J. Beerling gratefully acknowledges funding through a Royal Society University Research Fellowship and the Leverhulme Trust and J. A. Lake through a University of Sheffield Alfred Denny research studentship. R. A. Berner's research was supported by Department of Energy grant DE-FGO2-95ER14522 and National Science Foundation grant EAR-9804781. D. W. Taylor and L. J. Hickey gratefully acknowledge funding by a Chevron Oil Field Research grant, and D. W. Taylor thanks John M. Hayes for technical help and Carla Kinslow for assistance and acknowledges the Donors of The Petroleum Research Fund administered by the American Chemical Society for the partial support of this research.

Associate editor: B. E. Taylor

REFERENCES

- Arens N. C., Jahren A. H., and Amundson R. (2000) Can C_3 plants faithfully record the carbon isotopic composition of atmospheric carbon dioxide? *Paleobiology* **26**, 137–164.
- Beerling D. J. (1996) ^{13}C discrimination by fossil leaves during the late-glacial climate oscillation 12–10 kaBP: Measurements and physiological controls. *Oecologia* **108**, 29–37.
- Beerling D. J. and Berner R. A. (2000) Impact of a Permo-Carboniferous high O_2 event on the terrestrial carbon cycle. *Proc. Nat. Acad. Sci. U S A* **97**, 12428–12432.
- Beerling D. J., Woodward F. I., Lomas M. R., Wills M. A., Quick W. P., and Valdes P. J. (1998) The influence of Carboniferous palaeo-atmospheres on plant function: An experimental and modelling assessment. *Philos. Trans. R. Soc. London, Ser. B* **353**, 131–140.
- Berner R., Fogel M. L., Sprague E. K., and Hodson R. E. (1987) Depletion of ^{13}C in lignin and its implications for stable carbon isotope studies. *Nature* **329**, 708–710.
- Berner R. A. (2001) Modeling atmospheric O_2 over Phanerozoic time. *Geochim. Cosmochim. Acta* **65**, 685–694.
- Berner R. A. and Canfield D. E. (1989) A new model for atmospheric oxygen over Phanerozoic time. *Am. J. Sci.* **289**, 59–91.
- Berner R. A. and Kothavala Z. (2001) GEOCARB III: A revised model of atmospheric CO_2 over Phanerozoic time. *Am. J. Sci.* **301**, 182–204.
- Berner R. A., Petsch S. T., Lake J. A., Beerling D. J., Popp B. N., Lane R. S., Laws E. A., Westley M. B., Cassar N., Woodward F. I., and Quick W. P. (2000) Isotope fractionation and atmospheric oxygen: Implications for Phanerozoic O_2 evolution. *Science* **287**, 1630–1633.
- Berry J. A., Troughton J. H., and Björkman O. (1972) Effect of oxygen concentration during growth on carbon isotope discrimination in C_3 and C_4 species of *Atriplex*. *Carnegie Inst. Yearbook* **71**, 158–161.
- Bocherens H., Friis E. M., Mariotti A., and Pedersen K. R. (1994) Carbon isotopic abundances in Mesozoic and Cenozoic fossil plants: Palaeoecological implications. *Lethaia* **26**, 347–358.
- Cleveland W. S. (1979) Robust locally weighted regression and smoothing scatterplots. *J. Am. Stat. Assoc.* **74**, 829–836.

- Cope M. J. and Chaloner W. G. (1980) Fossil charcoal as evidence of past atmospheric composition. *Nature* **283**, 647–649.
- Draper N. R. and Smith H. (1983) *Applied Regression Analysis*. John Wiley, New York.
- Farquhar G. D. and Richards R. A. (1984) Isotopic composition of plant carbon correlates with water-use efficiency in wheat genotypes. *Aust. J. Plant Physiol.* **11**, 539–552.
- Farquhar G. D. and Wong S. C. (1984) An empirical model of stomatal conductance. *Aust. J. Plant Physiol.* **11**, 191–209.
- Farquhar G. D. and Lloyd J. (1993) Carbon and oxygen isotope effects in the exchange of carbon dioxide between terrestrial plants and the atmosphere. *Stable Isotopes and Plant Carbon-Water Relations* In: (eds. J. R. Ehleringer, A. E. Hall, and G. D. Farquhar), pp. 47–70. Academic Press, San Diego, CA.
- Farquhar G. D., Ehleringer J. R., and Hubrick K. T. (1989) Carbon isotope discrimination and photosynthesis. *Ann. Rev. Plant Physiol. Plant Mol. Biol.* **40**, 503–537.
- Farquhar G. D., O'Leary M. H., and Berry J. A. (1982) On the relationship between carbon isotope discrimination and the intercellular carbon dioxide concentration in leaves. *Aust. J. Plant Physiol.* **9**, 121–137.
- Garrels R. M. and Lerman A. (1984) Coupling the sedimentary sulfur and carbon cycles—An improved model. *Am. J. Sci.* **284**, 989–1007.
- Gillon J. S., Borland A. M., Harwood K. G., Roberts A., Broadmeadow M. S. J., and Griffiths H. (1998) Carbon isotope discrimination in terrestrial plants: Carboxylations and decarboxylations. *Stable Isotopes: Integration of Biological, Ecological and Geochemical Processes* In: (ed. H. Griffiths), pp. 111–131. Bios, Oxford, UK.
- Graham J. B., Dudley R., Aguilar N. M., and Gans C. (1995) Implications of the late Palaeozoic oxygen pulse for physiology and evolution. *Nature* **375**, 117–120.
- Hayes J. M., Strauss H., and Kaufman A. J. (1999) Abundance of ¹³C in marine organic matter and isotope fractionation in the global biogeochemical cycle of carbon during the past 800 Ma. *Chem. Geol.* **161**, 103–125.
- Holland H. D. (1978) *The Chemistry of the Atmosphere and the Oceans*. John Wiley, New York.
- Jones T. P. (1994) ¹³C enriched lower Carboniferous fossil plants from Donegal, Ireland: Carbon isotope constraints on taphonomy, diagenesis and palaeoenvironment. *Rev. Pal. Pal.* **81**, 53–64.
- Keeling C. D., Whorf T. P., Wahlen M., and van der Plicht J. (1995) Interannual extremes in the rate of rise in atmospheric carbon dioxide since 1980. *Nature* **375**, 666–670.
- Körner C., Farquhar G. D., and Roksandic Z. (1988) A global survey of carbon isotope discrimination in plants from high altitude. *Oecologia* **74**, 623–632.
- Körner C., Farquhar G. D., and Wong S. C. (1991) Carbon isotope discrimination by plants follows latitudinal and altitudinal trends. *Oecologia* **88**, 30–40.
- Lawlor D. W. (1993) *Photosynthesis: Molecular, Physiological and Environmental Processes*. Longman, Harlow, UK.
- Lenton T. M. and Watson A. J. (2000) Redfield revisited: 2. What regulates the oxygen content of the atmosphere? *Global Biogeochem. Cycles* **14**, 249–268.
- Lloyd J. and Farquhar G. D. (1994) ¹³C discrimination during CO₂ assimilation by the terrestrial biosphere. *Oecologia* **99**, 201–215.
- Mora C. I., Driese S. G., and Colarusso L. A. (1996) Middle to late Paleozoic atmospheric CO₂ levels from soil carbonate and organic matter. *Science* **271**, 1105–1107.
- Otto-Bliessner B. (1993) Tropical mountains and coal formation: A climate model study of the Westphalian (306 Ma). *Geophys. Res. Lett.* **20**, 1947–1950.
- Rachomilevitch S., Reuveni J., Pearcy R. W., and Gale J. (1999) A high level of atmospheric oxygen, as occurred toward the end of the Cretaceous period, increases leaf diffusion conductance. *J. Exp. Bot.* **50**, 869–872.
- Rees P. M., Gibbs M. T., Ziegler A. M., Kutzbach J. E., and Behling P. J. (1999) Permian climates: Evaluating model predictions using global palaeobotanical data. *Geology* **27**, 891–894.
- Robinson J. M. (1989) Phanerozoic O₂ variation, fire, and terrestrial ecology. *Palaeogeogr. Palaeoclim. Palaeoecol.* **75**, 223–240.
- Sage R. F. (1999) Why C₄ photosynthesis?. *C₄ Plant Biology* In: (eds. R. F. Sage and R. K. Monson), pp. 3–16. Academic Press, San Diego, CA.
- Turney C. S. M., Beerling D. J., Harkness D. D., Lowe J. J., and Scott E. M. (1997) Stable carbon isotope variations in northwest Europe during the last glacial-interglacial transition. *J. Quat. Sci.* **12**, 339–344.
- Veizer J., Ala D., Azmy K., Bruckschen P., Buhl D., Bruhn F., Carden G. A. F., Diener A., Ebner S., Goddérís Y., Jasper T., Korte C., Pawellek F., Podlaha O. G., and Strauss H. (1999) ⁸⁷Sr/⁸⁶Sr, δ¹³C and δ¹⁸O evolution of Phanerozoic seawater. *Chem. Geol.* **161**, 59–88.
- Valdes P. J. and Crowley T. J. (1998) A climate model intercomparison for the Carboniferous. *Palaeoclimates* **2**, 219–238.
- Van der Water P. W., Leavitt S. W., and Betancourt J. L. (1994) Trends in stomatal density and ¹³C/¹²C ratios of *Pinus flexilis* needles during last glacial-interglacial cycle. *Science* **264**, 239–243.
- Watson A. J., Lovelock J. E., and Margulis L. (1978) Methanogenesis, fires and the regulation of atmospheric oxygen. *Biosystems* **10**, 293–298.